Journal of Chromatography A 1767 (2026) 466644

Contents lists available at ScienceDirect

Journal of Chromatography A

journal homepage: www.elsevier.com/locate/chroma

Selectivity for full AAV capsids in affinity capture with camelid ligands

Lukas Bongers [a,*], Linda E. Franken [b], Dominik Hoch [a], Veronika E. Huber [a], Veronika Öttl [a], Elena B. Raaf [a], Jürgen Hubbuch [c], Roberto Falkenstein [a,1], Andres D. Martinez [a,1]

[a] Gene Therapy Technical Research & Development, Roche Diagnostics GmbH, 82377 Penzberg, Germany
[b] Roche Pharma Research and early Development, Roche Innovation Center Basel, Hoffmann-La Roche Ltd., 4070 Basel, Switzerland
[c] Department of Biomolecular Separation Engineering, Karlsruhe Institute of Technology, 76131 Karlsruhe, Germany

ARTICLE INFO

Keywords:
Gene therapy
Adeno-associated virus
Affinity chromatography
Full capsid selectivity
Camelid affinity ligands

ABSTRACT

The industry standard for downstream processing of adeno-associated viral vectors (AAV) is purification by affinity capture and anion exchange polishing (AEX). Affinity capture is an attractive method for capturing AAVs as it can remove process-related impurities and selectively enrich AAVs. Full capsids are then separated on AEX-resin from product related impurities based on net surface charge. Enrichment of full capsids remains a big challenge, as biophysical properties of full and empty capsids are very similar. We present a novel approach to enrich full capsids during capture chromatography using affinity resins. We examined the impact of additives (NaCl, $MgCl_2$, Na_2SO_4), NaCl concentrations (0 – 1000 mM), temperature and different affinity ligands (POROS™ CaptureSelect™ AAVX, AAV8, AAV9; CaptoAVB and AVIPure AAV8). We tested our approach for the serotypes AAV8 wild type (WT), AAV9 WT and an rAAV2 derivative and demonstrated 2.5-fold full capsid enrichment in a robotic screening. Analyzing an elution peak in fine increments yielded in multiple fractions approaching 100% full capsids. While several affinity resins demonstrated full capsid selectivity, we report that AAVX achieved the highest resolution. The selectivity was then linked to the affinity ligands specific binding mechanism towards an AAV capsid.

This novel capture method offers a trade-off between full capsid yield and purity without the need for additional unit operations while using an already established process. With enriched loading material for the subsequent anion exchange step, the polished elution pool has a higher full-to-total ratio (FTR) compared to a process based on standard affinity capture conditions.

1. Introduction

Adeno-associated viral vector-based gene therapies are gaining popularity, with seven drugs already approved by the FDA by September 2025. The delivery of exogenous genes in AAVs as delivery vehicles promises clinical success with high safety and efficacy compared to other delivery vehicles [1,2]. However, high costs of goods and substantial investments into research and development result in these drugs being cost-intensive, with prices reaching up to $3.2 million for a one-time infusion of Elevidys [3]. To keep the medication as affordable as possible it is crucial to lower costs and maximize product yield over the entire process.

Purification of AAVs is a critical bottleneck in the development of new AAV based gene therapies. As traditional purification by ultracentrifugation is not scalable, substantial effort has been invested into the development of chromatographic methods as a scalable, good manufacturing practice (GMP) compliant alternative [4,5]. Besides common process-related impurities such as host cell DNA and protein, purification deals with AAV capsids that are empty, partially filled or contain host cell DNA. These product related impurities are of concern as they increase the amount of AAV antigen presented and can cause an elevated immune response [6]. Known effects are an elevated innate immune response [7], increased counts of anti-AAV antibodies and triggered anti-capsid T-cell responses [8]. Additionally, it has been reported that lower full to total ratios (FTR) can decrease the overall transduction efficiency of AAV treatments [9,10]. These concerns

* Corresponding author.
E-mail address: lukas.bongers@roche.com (L. Bongers).
[1] equal contributors.

https://doi.org/10.1016/j.chroma.2025.466644
Received 14 November 2025; Received in revised form 16 December 2025; Accepted 19 December 2025
Available online 20 December 2025

highlight the importance of high FTRs in administered gene therapies.

Downstream processing for manufacturing typically consists of capture and polishing chromatography steps. The first unit operation, capture of AAVs with affinity resin, commonly uses commercially available camelid V_HH antibody fragments displaying high affinity towards capsids of different serotypes, depending on the ligand [11]. One of the most used resins for affinity-based capture is POROS™ CaptureSelect™ AAVX Affinity Resin (AAVX). Its popularity arises from high binding capacities reaching at least 1e14 capsids/mL for serotype AAVrH10 but up to >1e15 capsids/mL for the serotype AAV2 as well as from the affinity towards a wide range of capsids, including recombinant and chimeric vectors [12]. Other frequently used ligands are POROS™ CaptureSelect™ AAV8 (CSAL8) and POROS™ CaptureSelect™ AAV9 (CSAL9) resins by Thermo Scientific, Capto™ AVB (CaptoAVB) by Cytiva and AVIPure® AAV8 (AviPure) by Repligen.

Capture with one of the beforementioned affinity resins is conventionally performed in bind-and-elute mode. The resin selectively captures AAV capsids while process-related impurities are reduced. A drop in pH (pH ≤ 3.3) [13] will elute the concentrated capsid pool with yields ranging from 70–90 % depending on process optimization and the combination of serotype and affinity ligand [14].

The separation of empty, partial and full capsids is achieved with anion-exchange chromatography, in which charge variants can be separated. The observed separation is hypothesized to be caused by their different isoelectric points (IEP) [15–17]. However, capsid separation has been proven to be difficult as the difference in IEP is small (0.3–0.4) and because surface charge depends on capsid heterogenicity, surface topology, genome size and posttranslational modifications [18–20]. The FTR of material loaded onto an AEX-column directly impacts the chromatographic selectivity between full and empty capsids. Starting with a higher FTR can increase peak resolution and final FTR [21,22]. Considering this problem, new methods have been developed to maximize the enrichment factor of full AAVs, such as two-pass AEX [16] and weak-partitioning multi-column AEX [23]. However, even at high yields of individual unit operations, the overall process yield decreases significantly with the amount of additional process steps [13]. We investigated if it is possible to use common affinity capture to increase the FTR prior to polishing, which has previously been deemed impossible [21,24].

In this work, we demonstrate that lowering the pH in a linear gradient allows for the separation of full and empty capsids during affinity capture chromatography with commercially available resins, thereby utilizing an already widely used scalable unit operation without increasing the number of chromatography steps. By reducing empty capsids in the capture step, the product-related impurity-burden is reduced, allowing for smaller polishing columns with reduced buffer consumption or alternatively less polishing cycles per bioreactor. Peak resolution and purity of the final product are enhanced, mitigating potential immunogenic side effects for patients without drastically altering the already established platform for AAV purification.

2. Materials and methods

2.1. Material preparation

2.1.1. Production of AAV serotypes

All AAV serotypes used in this study were produced in-house through triple transfection processes. HEK293 suspension cells were cultivated in fed-batch mode, AAV-production was induced by adding a mix of plasmid media and transfection reagents. Cell lysis was induced according to a lysis protocol with Triton CG-110 (0.5 %), followed by the addition of Benzonase (50 U/mL) and incubation at 37 °C for 60 min [25]. Harvested cell culture fluid was clarified by depth filtration and 20x concentrated to reduce loading time for purification experiments. Concentrated cell culture fluid was aliquoted to avoid multiple freeze/thaw cycles and stored at −80 °C. The serotypes used in this study are AAV8 wild type (WT), AAV9 WT and a recombinant AAV2 (rAAV2). The 4.7 kb genome was of similar size and contained a gene coding for mGreenLantern (mGL) in all serotypes.

2.1.2. Material generation by standard affinity capture

After initial stripping, regeneration and equilibration (25 mM Tris/Tris–HCl, 0.15 M NaCl, 2 mM $MgCl_2$, 0.005 % P188, 1 % Sorbitol), 0.22 μm filtered concentrated cell culture fluid was loaded onto AAVX-resin at 5e14 capsids (cp)/mL resin at pH 7.4. Loading was followed by a second equilibration step and elution with 0.1 M Glycine-HCl, 2 mM $MgCl_2$, 0.005 % P188, pH 3.0. Collected material was immediately neutralized to pH 8.0 with neutralization buffer containing 1.5 M Tris. Eluting material was collected starting and ending at 10 mAU UV-absorbance at 280 nm (2 mm UV cell, Cytiva) to generate material with high yield at low dilution in elution Nbuffer. Column strip and regeneration are described in supplementary table S1.

2.1.3. Anion exchange polishing

Material purified by affinity capture was diluted in polishing buffer A (20 mM Tris/Tris–HCl, 2 mM $MgCl_2$, 0.005 % P188, 1 % Sorbitol, pH 8.0) to ensure binding. The material was 0.22 μm filtered and, after initial stripping, regeneration and equilibration at pH 8.0, loaded on Poros™ XQ strong anion exchange resin with a load density of 1e14 cp/mL resin. Loading was followed by a second equilibration step and elution with steps created out of a mixture of polishing buffer A and polishing buffer B (20 mM Tris/Tris–HCl, 2 mM $MgCl_2$, 200 mM NaOAc, 0.005 % P188, 1 % Sorbitol, pH 8.0). Eluting material was collected starting and ending at 10 mAU UV-absorbance at 280 nm (2 mm UV cell, Cytiva) to generate material with high yield at low dilution in elution buffer. Column strip and regeneration are described in supplementary table S1.

2.1.4. Full/Empty capsid separation by affinity capture

Experiments were carried out on an ÄKTA Avant 25 (Cytiva, MA, USA) equipped with standard pH, conductivity and UV-sensors. UV signals at 260 and 280 nm were monitored in every experiment and analyzed in Unicorn 7.10 (Cytiva). All investigated resins were used in prepacked 1 mL columns purchased from the respective manufacturer (Thermo Fisher Scientific for AAVX, CSAL8, CSAL9, Cytiva for CaptoAVB, Repligen for AviPure). AAV load material was thawed in a waterbath at 25 °C and filtered with Minisart 0.22 μm 6.2 cm^2 syringe filters (Göttingen, DE) prior to loading. Buffers are described further in supplementary table S2. The chromatography method is described in supplementary table S3. To ensure comparability between runs, high yield and low dilution in elution buffer, peaks were collected fully and not fractioned into small increments. The experiment described in Fig. 1 is the only exception. Here, the elution peak was divided into increments of 1 column volume (CV) each to do a detailed analysis of the material eluting at different sections in the peak. Every elution peak was collected starting and ending at 10 mAU UV-absorbance at 280 nm (2 mm UV cell, Cytiva).

2.2. Analytical methods

2.2.1. Electrochemiluminescence immunoassay

Total capsid titer was measured with an Electrochemiluminescence immunoassay (ECLIA) on a cobas pro e801 device (Roche Diagnostics, Penzberg, GE). Based on the sandwich principle, a serotype specific monoclonal antibody was bound to the AAV and to a secondary antibody, which formed a complex with a magnetic particle. The microparticles were fixed to the surface of an electrode by magnetic action and unbound substances were removed. By applying voltage, chemiluminescent emission was induced and measured with the photomultiplier. Results were determined based on a calibration curve with known concentrations of AAV. A relative standard deviation of 10 % was observed.

2.2.2. Digital polymerase chain reaction

Full capsid titer was measured with digital polymerase chain reaction (dPCR) on a Qiacuity Eight System (Qiagen, Hilden, DE). AAV samples were first treated with nuclease to remove free nucleic acids outside the particles. To release the viral genomes, capsids were subsequently digested with Proteinase K. A dPCR master mix containing a FAM-labeled primer/probe stock solution and restriction enzyme SmaI was prepared with the QIAcuity Probe PCR Kit (Qiagen) and diluted and measured according to the manufacturer's instructions. Results were evaluated with the QIAcuity Software Suite 2.5.0.1. The analysis yielded a relative standard deviation of 10 % in agreement with existing literature [26].

2.2.3. High performance liquid chromatography

Determination of relative hydrophobicity and comparison of elution pH on AEX-resin was performed on an Agilent Technologies 1290 Infinity II LC system (Santa Clara, CA, USA) consisting of a high-speed binary pump (G7120A), a multisampler set (G7167B) with a 20 µL sample loop, a column compartment set to 22 °C (G7116B), a UV-detector (G7114B) and a 1260 Infinity fluorescence detector (G1321B) in the order as presented. The UV-detector operated at 260 nm and 280 nm. The fluorescence detector was operated at a PMT gain of 12 with excitation at 280 nm and emission detection at 330 nm and 350 nm.

Relative hydrophobicity measurements were performed with a TSKgel Ether-5PW HPLC column, 10 µm (Tosho Bioscience, Tokyo, Japan). 20 µL of sample were applied to a gradient from 100 % eluent A (20 mM Tris, 2 M ammonium sulfate pH 7.5) to 100 % eluent B (20 mM Tris, pH 7.5) and a constant reduction in ammonium sulfate of 50 mM/min at a constant flow rate of 0.8 mL/min after equilibrating the column in eluent A for 2 min. The method was based on previous work with mAbs [27] and has been optimized for AAVs. AAVs were detected with fluorescence as this detection method is more sensitive than UV [28]. Retention times of rAAVs were determined at the peak apex.

AEX elution pH were obtained with a CIMac AAV empty/full – 0.1 mL column, 1.3 µm (Sartorius BIA Separations, Ajdovscina, Slovenia). As the HPLC itself did not have a pH-probe, the buffer system was tested for linearity in the pH-gradient with an Äkta Avant 25 first. Elution pH was calculated based on initial pH-values of the buffer system and the retention time. Retention time was measured at the peak apex. Samples were prepared by affinity chromatography and diluted 1:10 in eluent A to ensure binding. Eluent A contained 20 mM Bis-Tris-Propane (BTP), 20 mM 2-(N-morpholino)ethanesulfonic acid (MES), 2 mM $MgCl_2$ at pH 9.0 (rAAV2, AAV8 WT) or pH 9.5 (AAV9 WT). After 2 min of equilibration in eluent A, 100 uL of sample were applied and eluted in a linear gradient from 100 % eluent A to 100 % eluent B (20 mM BTP, 20 mM MES, 2 mM $MgCl_2$ at pH 5.5 (rAAV2, AAV8 WT) or pH 7.5 (AAV9 WT) at a pH-reduction rate of 0.1 pH / min and a constant flow rate of 1 mL/min. Retention times were determined at the respective peak maxima. Buffer systems were developed based on previous work utilizing salt gradients with the same resin [29] and by combining buffer species with a pK_a in the required buffering range [30].

2.2.4. Batch screening

A batch screen in a Tecan Fluent 1080 system (Tecan Group, Männedorf, Switzerland) was used to evaluate the elution behavior of full and empty capsids at different pH and salt molarity conditions (software Fluent Control). The system was equipped with Robotic Gripper Arms™ (RGA) with eccentric and centric gripper fingers respectively, Flexible Channel Arms™ (FCA) for air and liquid respectively, a Tecan Carousel HS for plate storage, a Rotanta 460 Robotic centrifuge and a Tecan BioShake for mixing. Titers and FTRs were measured with an integrated Tecan Spark (Software Magellan). The Tecan Spark measured capsid titer with fluorescence, excitation at 280 nm and emission at 350 nm. The FTR was calculated with the ratio of 260 nm and 280 nm.

A filter plate (96 multi-well plates, Acroprepadv™ 1 mL, 0.45 µm, Polypropylen, Pall Corporation, New York, NY, USA) containing 50 µL of CS AAVX-resin per well was divided into 2 halves, where one-half received a pool with previously enriched full capsids (AEX full pool, FTR = 66 % by Tecan Spark) at a load density of 1e14 cp/mL resin, the other half received a pool of previously enriched empty capsids (AEX empty pool, FTR = 5 % by Tecan Spark) with the same load density. A total of 48 buffer conditions, eight salt concentrations and six pH values, were analyzed for their effect on full/empty capsid separation and viral genome (vg)-yield. The full capsid (FC)-enrichment was calculated as the FC-yield of the previously enriched FC-pool divided by the cp-yield of the previously enriched empty capsid (EC)-pool. As FCs make up for only 5 % in the EC-pools, they were disregarded in the calculation.

Buffers for all pH-values with the lowest and highest salt concentration were prepared manually and sterile filtered. Intermediate salt concentrations were prepared by the Tecan Fluent. All buffers contained 100 mM formic acid, 2 mM $MgCl_2$, 0.005 % P188 and NaCl according to the respective concentration. The pH was adjusted by titration with 10 M NaOH. Buffers were adjusted to pH 3.8 – 3.3 in 0.1 pH increments with salt concentrations that equal a conductivity of 15 – 50 mS/cm in 5 mS/cm increments.

Execution of the batch screen consisted of an initial resin strip (described in supplementary table S1) and regeneration followed by two equilibration steps (20 mM Tris/Tris–HCl, 2 mM $MgCl_2$, 0.005 % P188, pH 7.4). Subsequently, load was applied in a total of three steps, followed by equilibration, two elution steps in the respective elution buffer and stripping. Every step consisted of the application of 300 µL liquid volume and centrifugation. The liquid flow-through of every step was collected and analyzed by the Tecan Spark.

2.2.5. Evaluation software

Chromatograms and Batch-Screen results were evaluated in MATLAB R2019a. Data is presented with Excel 365, BioRender and MATLAB R2019a.

3. Results and discussion

Production of AAVs using the triple transfection protocol commonly results in FTRs of 15 % - 30 % [31]. This poses a challenge for subsequent downstream processing, especially as the separation and FC enrichment factor of anion exchange chromatography are limited and dependent on the FTR of the load [32]. In this paper we demonstrate the possibility of increasing the FTR of an AAV pool by affinity capture with camelid ligands. Conventionally, elution of AAV capsids bound to the affinity resin takes place at pH $\leq$ 3.3 as discussed previously, maximizing the yield while maintaining acceptable product quality. In this case the FTR of the elution pool remains unaffected [33]. When lowering the pH in a gradient instead, we found that FCs for all serotypes tested showed lower affinity to several camelid-based affinity resins. Consequently, FCs eluted earlier during the pH-gradient and were effectively separated from ECs, challenging the prevailing view that the resins tested in this work lack selectivity between FCs and ECs [21,24]. This work solely utilized pH-gradients, as changes in the elution behavior are better observable in a gradient than in a step elution. However, for manufacturing processes, a step elution with fixed conditions is preferrable as gradients pose several challenges such as high buffer consumption and unrobust processes due to insufficient inline mixing [34].

3.1. Full capsid enrichment during AAVX pH-Gradient elution

The use of POROS™ CaptureSelect™ AAVX affinity resin allows for the partial separation of full capsids from empty capsids. As indicated in Fig. 1a, the pH was gradually lowered in a linear gradient with a constant change of 0.1 pH per column volume (CV) and with 5 CV holding steps at 0 and 100 % of the gradient. The different elution profiles of ECs and FCs are indicated by the different UV-absorbance profiles. While proteins, and thus the capsid, preferentially absorb light at a wavelength

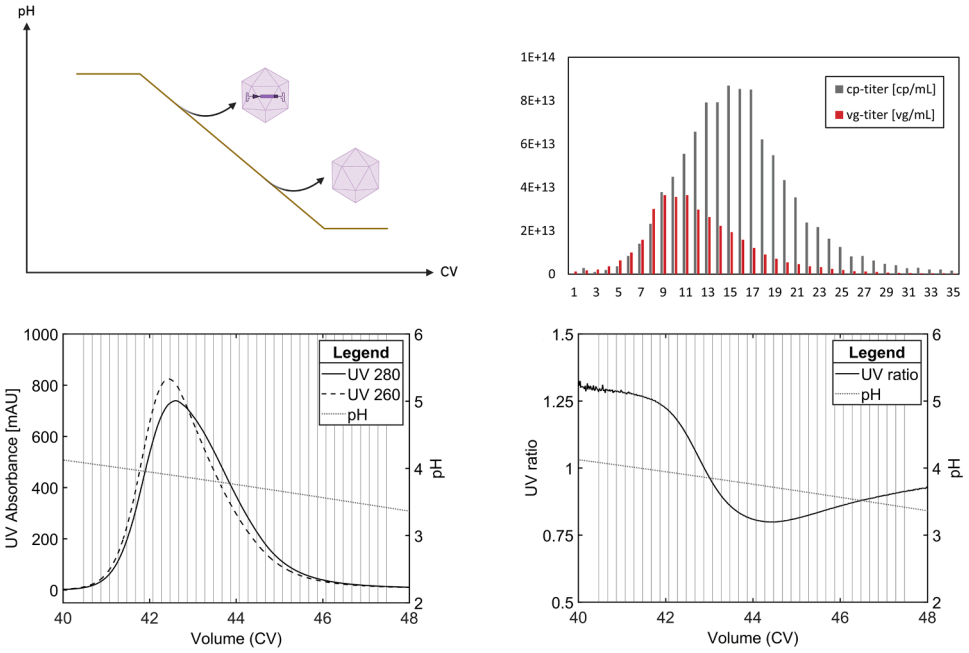

Fig. 1. Exemplary full/empty capsid separation on CaptureSelect AAVX-resin. Fig. 1a: Graphical depiction of capsid separation in a pH-gradient. Fig. 1b-1d show results from the same chromatography experiment. AAV8 WT was loaded onto a 5 mL column and eluted in a pH-gradient (detailed information in the supplementary tables). Fig. 1b shows the absorbance at 260 and 280 nm, resulting in the 260/280-ratio depicted in Fig. 1d Fig. 1c shows the titers corresponding to the respective fractions marked by vertical lines in the chromatogram.

of 280 nm, DNA (thus the viral genome) displays maximal absorbance at 260 nm [35]. It is therefore feasible to use the ratio of the UV260/UV280 absorbance to determine the FTR of an elution pool [29]. The dual-wavelength chromatogram (Fig. 1b) was used to calculate a UV absorbance ratio (Fig. 1d). While empty capsids have a UV absorbance ratio of around 0.6, a pool with 100 % full capsids can have a ratio of up to 1.4, depending on amino acid content, transgene composition and transgene length [36]. However, accuracy can be compromised by process-related impurities such as host cell proteins. To address this uncertainty, an elution peak was collected in fine increments. Each fraction was subsequently analyzed for its FC and total capsid titers using dPCR and ECLIA, allowing for the calculation of a FTR. A 5 mL column was loaded with 1e15 AAV8 WT capsids, resulting in a load density of 2e14 capsids / mL (cp/mL) resin, the load material had a FTR of 35 %. Capsids were eluted with citric acid in a pH-range of 6.0 to 2.5. Detailed information on process conditions is provided in supplementary table S2. The elution peak was fractionated in a total of 35 fractions as indicated by the vertical lines. While the pH-gradient did not achieve baseline separation, Fractions 1–8, eluting at pH 4.10 to 3.97, contained a high relative number of FCs, shown by a UV-ratio of 1.285 (fraction 1), which then decreased to 1.250 in fraction 8. Titer measurements with dPCR/ECLIA additionally indicated 100 % FCs in fractions 1–8. The trend towards decreasing FTR observable in the UV-ratio was masked by the deviation of the analytical assays. The crossover of both UV wavelengths, marked by UV-ratio = 1, was reached in fraction 13. Most FCs already eluted at higher pH; fraction 13 had a FTR of 33 %. The FTR then continued to drop to a lower limit of 13 % in fraction 21 with a corresponding UV-ratio of 0.80. Interestingly, the FTR then increased again towards the end of the elution peak with a second crossover reached in fraction 33. However, the titer in these late eluting fractions was comparably low, the count of FCs was minimal with vg-titers dropping below 1e12 vg/mL in fraction 29 after ranging as high as 3.6e13 vg/mL in fractions 9–11.

After an initial scouting with citric acid that allows for a wide buffering range, the buffer species was exchanged as the high conductivity of citric acid consequently requires large dilution volumes for preparing subsequent anion exchange load material. Glycine is amongst the most common buffer species used for affinity capture of AAVs [12,14,37,38]. AAV9 however eluted in the range of pH 4.6 to 4.0 (Fig. 2b), thus outside the buffering range of glycine. With a pK_a of 4.76, acetate is a suitable buffer species for the required elution pH-range of this serotype. As the elution pH of rAAV2 and AAV8 WT were in the range of pH 3.0 to 4.0, we proceeded with formic acid (pK_a 3.77) and decided against acetate or glycine in this case, as both do not buffer in the full pH-range required. The elution pH, determined at the UV280 peak apex for AAV8 WT, differed marginally between citric acid (pH 3.88) and formic acid (pH 3.63) in an otherwise equal buffer matrix.To assess FC/EC separation for three serotypes, we defined the elution buffer as 100 mM of a main buffer species depending on the elution pH with additional 200 mM NaCl (additional information in supplementary table S2). Out of the tested molarities, 200 mM of NaCl was determined the most preferential for FC/EC separation of AAV8 WT capsids due to the enhanced selectivity between FCs and ECs (Fig. 3c-d) and consequently was used for all serotypes to ensure comparability. AAV8 eluted from pH 3.9 to 3.3 (Fig. 2a), rAAV2 had the most acidic elution requirements with pH 3.6 to 3.0 (Fig. 2c) at identical buffer compositions. Selectivity and efficiency of the elution were highly serotype-dependent (Fig. 2a-c). The elution peak of AAV9 WT was wider than for rAAV2 and AAV8 WT, which both fully eluted within 4 CV at fixed pH-gradient speed. The UV-ratio profiles for serotypes rAAV2 and AAV9 WT were very comparable, starting at UV260/UV280-ratio = 1.25 with a crossover of both UV-signals at 3 CV and a total elution over 4–6 CV. AAV8 WT showed a steeper drop of the UV 260/280 ratio over the elution (Fig. 2d), hinting towards higher selectivity but also potentially lower process robustness due to higher pH-sensitivity. This observation may be attributed to differences in non-conserved amino acid sequences altering surface topology at the affinity ligands binding site, although futher evidence is required to confirm this mechanism. As selectivity was highest for AAV8 WT, this serotype was chosen to further study the impact of different ion types and concentrations on the separation.

In a first set of experiments, we analyzed the effect of different buffer excipients on selectivity and yield for AAV8 WT based on their respective position in the Hofmeister series. Sodium sulfate (Na_2SO_4) is a strong cosmotrope [39] and was expected to increase binding strength

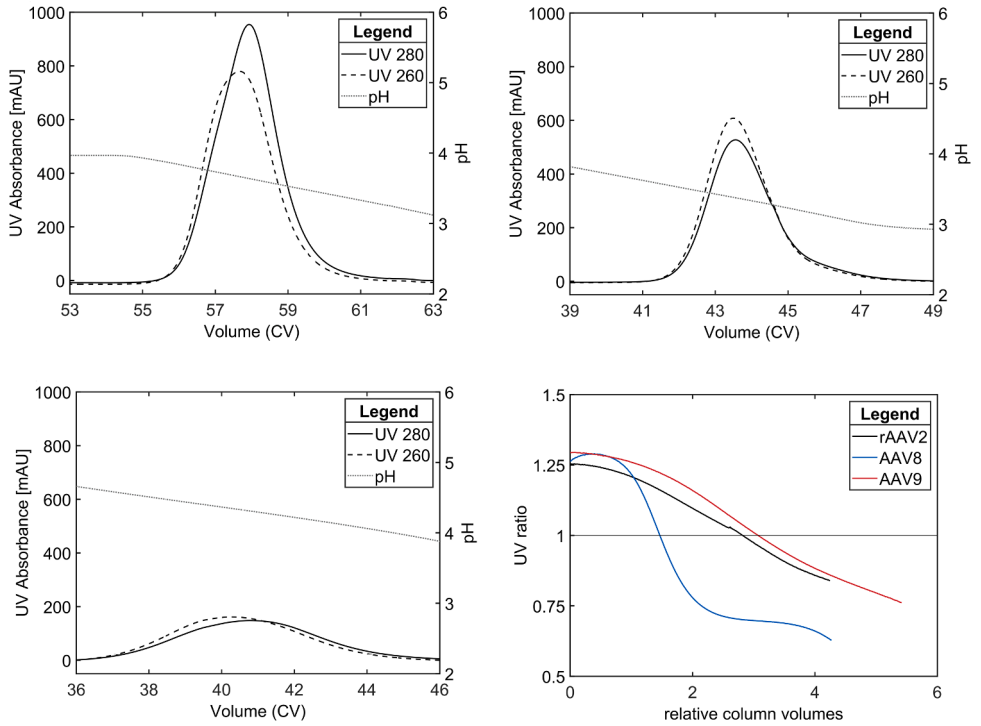

Fig. 2. Shown is the UV-signal at the wavelengths 260 and 280 nm of elution peaks in a pH-gradient from 10 mAU to 10 mAU (2 mm UV-cell, Cytiva) for AAV8 WT (Fig. 2a), AAV9 WT (Fig. 2b) and rAAV2 (Fig. 2c). Detailed information can be found in supplementary tables S1-S3. Fig. 2d shows the corresponding UV-ratios. Relative column volumes are defined as the column volumes of the elution peaks from 10 mAU to 10 mAU.

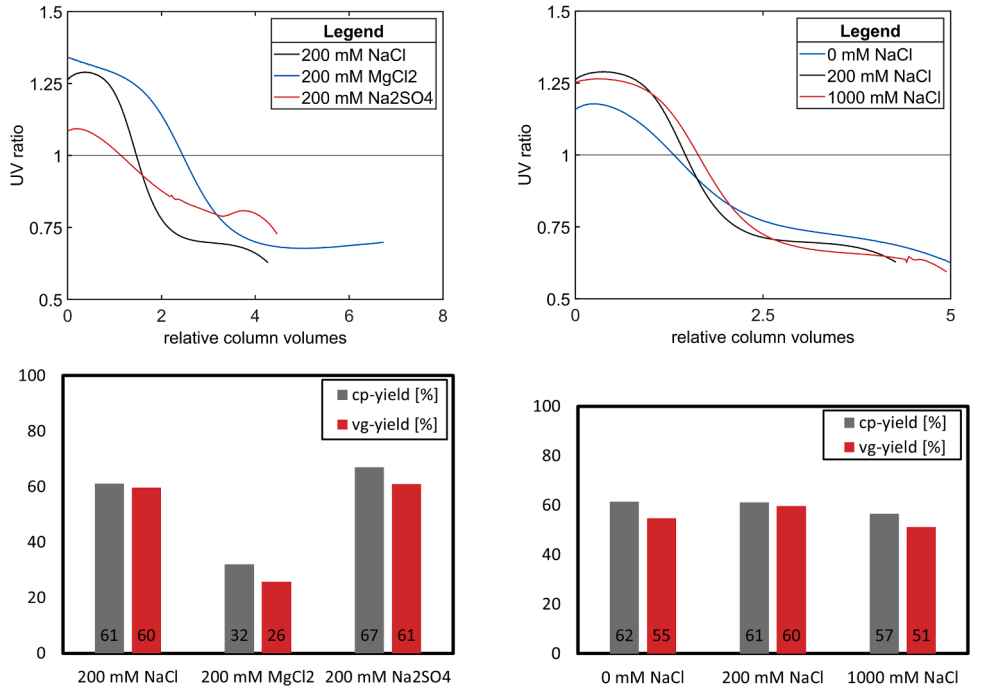

Fig. 3. AAV8 WT was bound to and eluted from CaptureSelect AAVX-resin in a pH-gradient with elution buffers that contained different excipients (Fig. 3a-b) or NaCl at different concentrations (Fig. 3c-d). Relative column volumes are defined as the column volumes of the elution peak from 10 mAU to 10 mAU.

compared to more moderate or chaotropic salts by enhancement of hydrophobic interactions between capsid and ligand. Sodium chloride (NaCl) is a popular eluent in anion exchange chromatography and known as a weak cosmotrope [40]. Magnesium chloride ($MgCl_2$) was included in this study as it is a common excipient in anion exchange chromatography, known to enhance selectivity between full and empty capsids [41]. NaCl and Na_2SO_4 showed comparable viral genome (vg)-yields (Fig. 3b). An elution buffer with 200 mM $MgCl_2$ decreased cp and vg-yield by 50 %, making it the least favorable condition. FC/EC capsid separation was however observed with every condition tested.

As the addition of NaCl led to comparable yields but higher selectivity than Na_2SO_4, we continued testing with different concentrations

of NaCl in otherwise equal conditions. While the obtained yields were around 60 % and did not change significantly between the experiments described above (Fig. 3d), the elution pH was highly dependent on the salt concentration. We observed that AAV8 WT capsids elute at the comparably highest pH in an elution buffer that did not contain Na^+ or Cl^- ions except for the ions needed to adjust the pH accordingly (pH 4.1 – 3.4). The addition of NaCl led towards a decrease in elution pH in a non-linear manner (200 mM NaCl: pH 3.9 – 3.3, 1000 mM NaCl: pH 3.6 – 2.8). Selectivity between full and empty capsids was reduced in elution buffer witout additional NaCl. There was no significant difference in selectivity between 200 and 1000 mM NaCl (Fig. 3c). Out of the conditions tested, 200 mM NaCl was therefore the most beneficial, as it combined superior resolution with high elution pH. However, polishing with AEX-resin relies on low conductivity of the load material to ensure capsid binding [32]. It is therefore crucial to determine an ideal salt concentration for the elution buffer.

After confirming the positive influence of NaCl on FC/EC selectivity (Fig. 3c-d), more refined increments in NaCl-concentrations and pH were screened utilizing a Tecan liquid handling system. The lowest salt molarity tested was 64 mM NaCl, equaling a conductivity of 15.0 mS/cm, while the highestconcentration tested was 460 mM NaCl, calculating to 50 mS/cm. To determine ideal separation conditions, the FC enrichment was calculated as described in Section 2.2.4. Selectivity was maximized for the highest molarity and pH tested (460 mM NaCl, pH 3.8). While the salt concentration contributed to the selectivity, the influence of pH was striking and exhibited a high degree of sensitivity. A decrease from pH 3.7 to pH 3.6 at 460 mM NaCl caused a reduction of the FC enrichment factor from 1.80 to 1.22 (Fig. 4a). In contrast, reducing the salt molarity to 100 mM at a constant pH of 3.7 resulted in adecline from 1.80 to 1.59.

Determining the vg-yield in FC containing wells of the plate revealed an inverse proportionality to the FC enrichment factor (Fig. 4b). While minor fluctuations in the low pH / low conductivity area were possibly caused by instrumental deviations, low pH and little to no salt appeared ideal for high vg-yields around 75 % under the given conditions. For the most favored separation condition, the vg-yield demonstrated a minimum at 42 %. A high selectivity is therefore achieved at a trade-off in vg-yield as also indicated in Fig. 1c (FTR = 100 % at 15 % vg-yield). In a step gradient elution developed for manufacturing scale, capsids remaining on the column after the first elution step would be eluted in a subsequent elution step or column strip. This material is either lost or has to be combined with fresh harvest material to achieve increased FC-recovery.

To select a preferred salt molarity and pH for FC-enrichment, several factors must be considered. Depending on the serotype, a minimal ionic strength can be necessary to prevent aggregation [42]. Low pH may additionally increase attraction between capsids and cause reversible aggregation [43]. While it has been hypothesized that low pH can diminish biological activity of the vector [44], thorough testing with AAV5, 8 and 9 has confirmed a stable potency in acidic conditions, presuming immediate neutralization after elution [45]. Higher salt concentrations also cause prolonged loading time for anion exchange chromatography as low conductivity is required for capsid binding. The inferred longer hold-time on the AEX-resin can alter capsid stability, shift retention times and decrease resolution between FC and EC [29]. Independent of the ionic strength, our data suggests that pH is the main driver behind FC/EC-separation during capture.

3.2. Resin-dependent capsid separation

The affinity ligand plays a crucial role in the resolution between full and empty capsids. Depending on the serotype, we compared different resins to AAVX. Yield was determined by collecting the entire elution peak in one fraction from 10 mAU to 10 mAU (2 mm UV cell, Cytiva). Buffers, column size and load density were identical between experiments with one serotype. For the affinity capture of rAAV2, AAVX was compared with CaptoAVB (Fig. 5a). Notably, binding strength between capsid and ligand was lower for CaptoAVB as capsids eluted at higher pH (Apex UV280 = 3.85) compared to AAVX (Apex UV280 = 3.43). The selectivity achieved with CaptoAVB was slightly reduced compared to AAVX as evident by the minimal / maximal UV-ratio during the elution (1.25–0.95, CaptoAVB and 1.27 – 0.9, AAVX). With CaptoAVB-resin, capsids eluted over 9.5 CV and thus over a wider pH-range compared to AAVX (4.5 CV), enabling higher control of separation in steps and increasing process robustness. With CaptoAVB, we achieved 14 % higher cp- and vg-yield (Fig. 5c), making it the favorable choice for rAAV2 capture and capsid separation under the conditions tested.

For AAV8 WT, AAVX was compared to CSAL8 and AVIPure AAV8 resin (Fig. 6a). A pH-gradient with AVIPure AAV8 resin resulted in a UV-ratio that started out at 1.1 and then quickly decreased to 1 (Fig. 6b), indicating a FTR of approximately 33 %. It remained constant over the entire capsid elution, showing strongly reduced selectivity while resulting in similar yields compared to AAVX. Capsid elution on CSAL8 resulted in a total of four crossovers of UV260/UV280. Compared to AAVX-resin, the selectivity was strongly diminished. The yield was 10 % higher compared to AAVX and AviPure AAV8 (Fig. 6c), further supporting the previously discussed trade-off in capsid separation. Out of the three resins tested, the elution pH was highest for AAVX (Apex UV280 = 3.88). With the process conditions used here, CaptoAVB did not bind AAV8 WT capsids (data not shown).

AAVX was compared to CSAL9 for serotype AAV9 WT (Fig. 7a). Capsid-yield was 15 % higher for CSAL9 resin, vg-yield was measured 12 % higher (Fig. 7c). Interestingly, the UV-ratio for CSAL9-resin started below 1, suggesting that a initial fraction of empty capsids could be removed in a wash step (Fig. 7b). The capsids then eluted in two peaks without reaching baseline separation. While the first peak contained

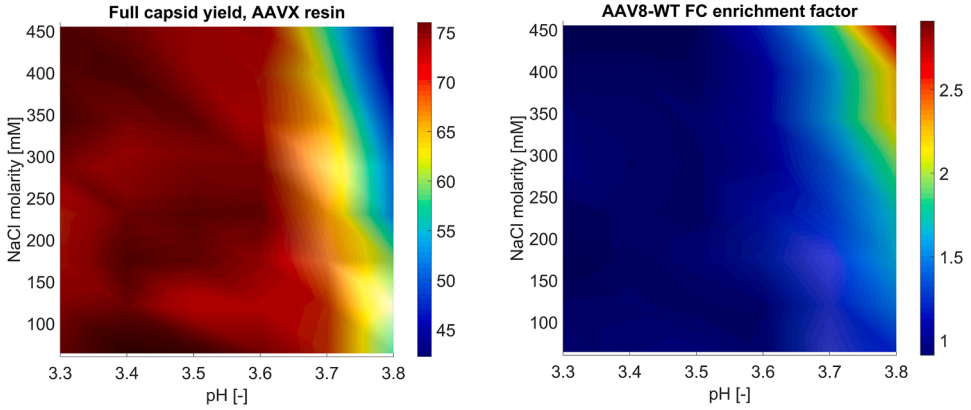

Fig. 4. Batch-Screen data. Fig. 4a depicts the FC enrichment per condition tested, Fig. 4b shows the corresponding vg-yield.

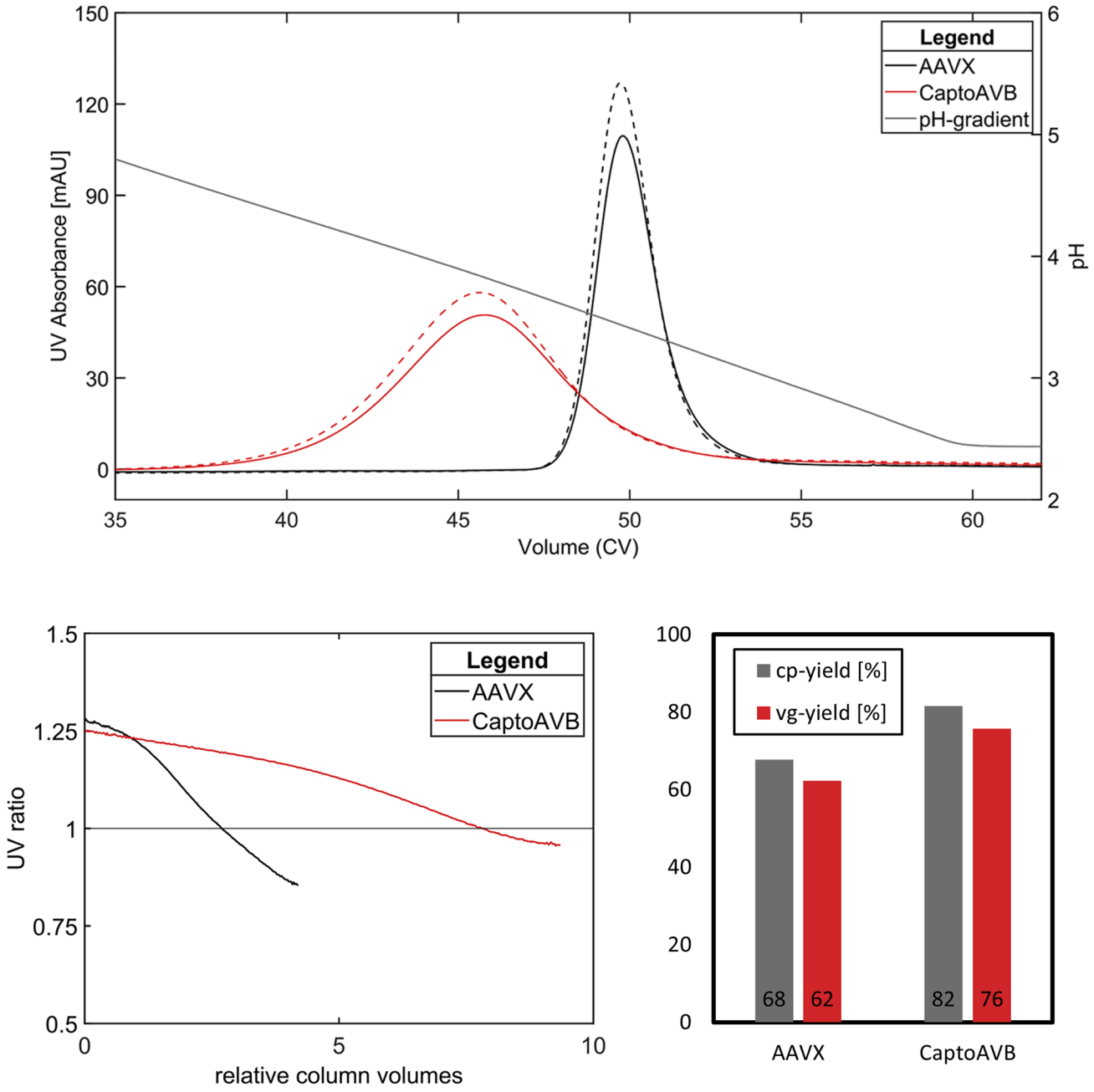

Fig. 5. Comparison of CaptureSelect AAVX-resin and CaptoAVB-resin with rAAV2. Fig. 5a shows the pH-gradient (grey), and the elution peak for the respected resin with 260 nm (–) and 280 nm (–). Fig. 5b shows the corresponding UV-ratios from 10 mAU-10 mAU. Relative column volumes are defined as the column volumes of the elution peak from 10 mAU to 10 mAU.

more full capsids than the second peak, overall FC/EC selectivity was less pronounced than on AAVX-resin. The underlying mechanismn responsible for the formation of two peaks has still to be determined.

In summary, while initially observed for AAVX-resin, we found that several camelid-derived affinity-resins have different affinity for full versus empty capsids. The selectivity was highly ligand-dependent and is, to this point, not predictable. While every ligand caused a shift in the UV-ratio over the elution peak, the effect differed as indicated in Table 1. AVIPure AAV8-resin displayed reduced separation of FCs from ECs (Fig. 6b). CSAL8-resin separated capsids in a unique manner that led to four crossover points and two peaks in the UV-ratio. While CSAL8 achieved the highest yield under the conditions tested, full AAV8 WT capsids were, just like with AVIPure AAV8, not as effectively enriched. CSAL9 enriched FCs similar to AAVX but at lower selectivity and efficiency (Fig. 7b-c). Considering the significantly higher process yield compared to AAVX-resin, it can still be a viable option to obtain an initial enrichment with CSAL9-resin to generate enriched loading material for the anion exchange step.

Of the resins tested, CaptoAVB-resin performed the most comparable to AAVX (Fig. 5b). Capsid elution initially exhibited highly enriched FCs; the ratio then slowly decreased until the elution pool almost entirely consisted of product related impurities in the tailing section of the peak. The reported cp- and vg-yields for CaptoAVB were 14 % higher than for AAVX. While the elution was less efficient, thus causing dilution of the elution pool, the same effect can promote higher process robustness in a step gradient elution.

For the beforementioned affinity resins, 3-dimensional structures are known. CryoEM confirms that the AAVX-ligand is structurally almost

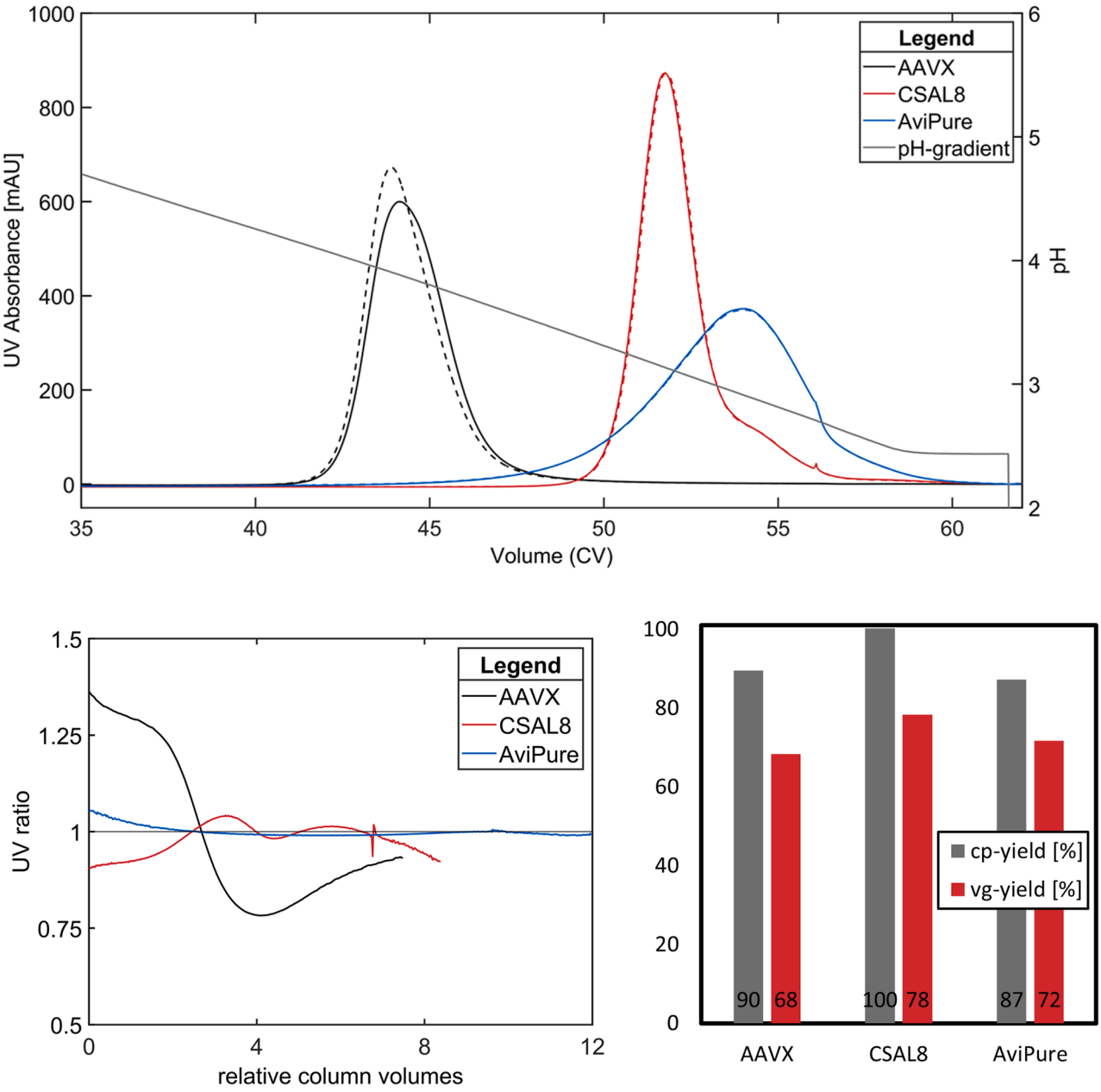

Fig. 6. Comparison of CaptureSelect AAVX-resin, CaptureSelect AAV8-resin and AviPure AAV8-resin with AAV8 WT. Fig. 6a shows the pH-gradient (grey), and the elution peak for the respected resin with 260 nm (–) and 280 nm (–). Fig. 6b shows the corresponding UV-ratios from 10 mAU-10 mAU. Relative column volumes are defined as the column volumes of the elution peak from 10 mAU to 10 mAU.

identical to the CaptoAVB-ligand, possibly explaining the highly comparable elution behavior. AAVX and CaptoAVB-ligand bind to the capsid around the 5-fold axis with an almost perfect overlap. While CaptoAVB resin binds five ligands per capsid, AAVX binds on average with only two units per capsid [46]. CSAL9 also binds near the 5-fold axis but has a different structural conformation than AAVX and AVB, potentially giving reason for the deviating capsid separation. Out of the ligands tested, CSAL8 is the only resin binding to the side of the 3-fold protrusions and the 2/5-fold wall [14]. AVIPure AAV8 ligands bind to the outside tip of the 3-fold protrusions [47]. A comparison of all serotypes and affinity ligands investigated can be found in Table 1. In conclusion, while none of the tested ligands had a constant UV-ratio over the entirety of a pH-gradient elution, only the ones that bind near the 5-fold channel, which is known to be involved in the active transgene packaging, showed elevated FC/EC separation [48,49].

We suggest molecular docking simulations to simulate the differences in binding forces between full/empty capsids and ligands and to gain more insight into the affinity mechanisms described here.

3.3. *Influence of temperature on yield and full/empty selectivity*

Hydrophobic interactions as well as diffusion are influenced by temperature. In an ambient temperature range (0–37 °C), lower temperature results in lower hydrophobic interactions [50] and reduced mass transfer kinetics [51,52]. As affinity is a complex interplay of different binding mechanisms, we tested the effect of temperature on AAV-elution on AAVX-resin. The experimental setup was identical to the runs shown above, however, the column was submerged in a temperature-controlled waterbath. It should be noted that the pH-probe in the Äkta25-system is installed behind the column, UV-cell and

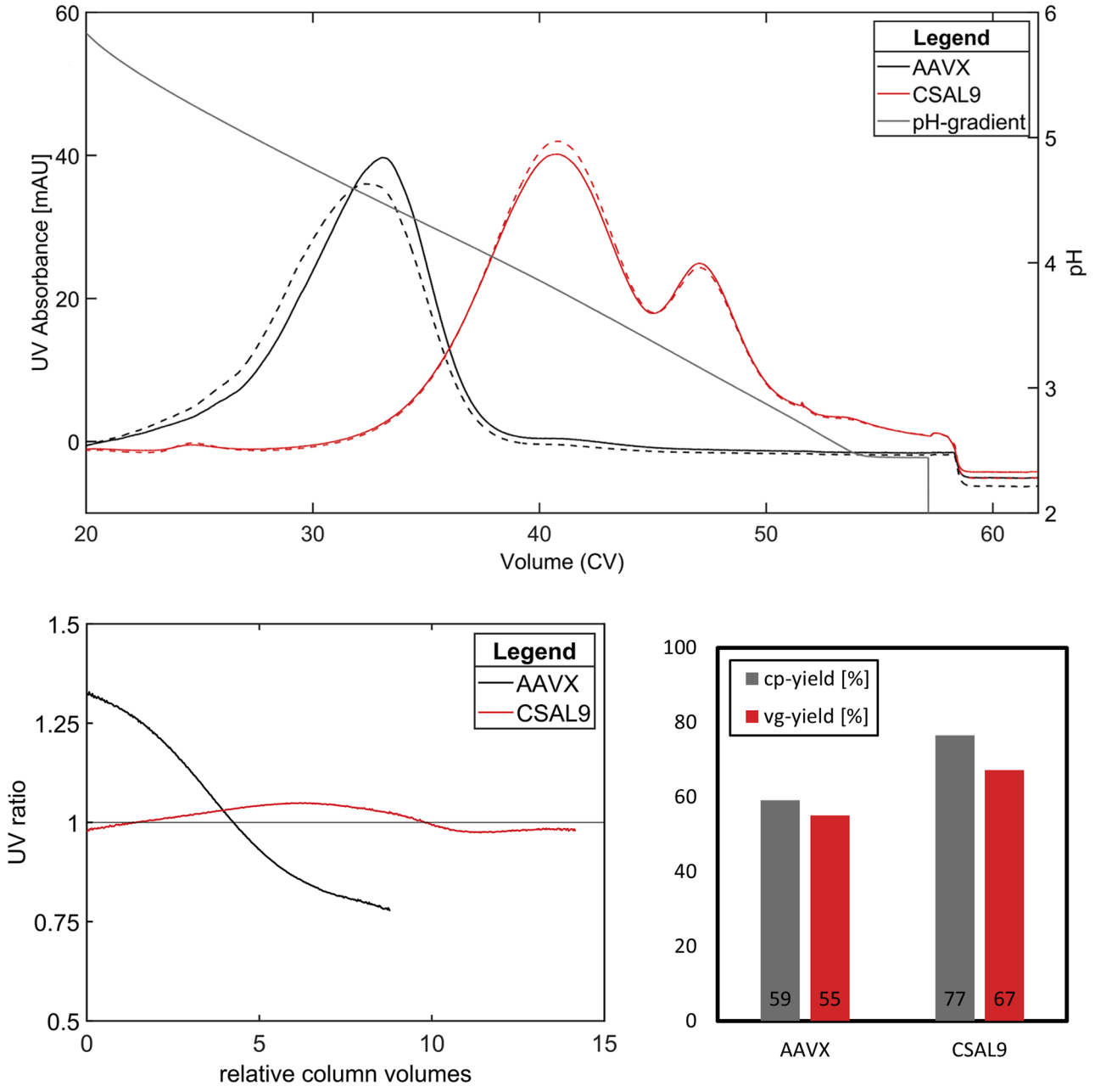

Fig. 7. Comparison of CaptureSelect AAVX-resin and CaptureSelect AAV9-resin with AAV9 WT. Fig. 7a shows the pH-gradient (grey), and the elution peak for the respected resin with 260 nm (–) and 280 nm (–). Fig. 7b shows the corresponding UV-ratios from 10 mAU-10 mAU. Relative column volumes are defined as the column volumes of the elution peak from 10 mAU to 10 mAU.

Table 1
Summary of Retention Behavior of AAVs on different Camelid Affinity Ligands during a pH-gradient elution ranked by FC/EC resolution with AAVX being ranked highest.

Affinity Resin	Serotype	Ligand binding site
AAVX	rAAV2, AAV8, AAV9	5-fold pore
CaptoAVB	rAAV2	5-fold pore
CSAL9	AAV9	5-fold pore
CSAL8	AAV8	2/5-fold wall
AviPure AAV8	AAV8	3-fold protrusion

conductivity probe. Buffers were not pre-tempered as the time the mobile phase spent in a column-inlet tubing within the water bath was sufficient to adjust the temperature. When using small columns with low flow rates, the mobile phase returns back to room temperature by the time it reaches the pH-probe, potentially resulting in a pH different from that within the temperature-controlled column. We therefore directly measured the buffer at the respective temperature and found only a small deviation. The buffer measured resembled the buffer matrix at the UV280 apex of AAV8-elution at 25 °C. At 25 °C, the measured pH was 3.67. The pH decreased to 3.66 at 37 °C and increased to 3.68 at 10 °C and 3.73 in an icebath at approximately 0 °C. This temperature-mediated pH shift is smaller than the observed shift in capsid elution and enhances the observed effect, as the pH measured offline and the elution pH (measured at 25 °C) both increased at lower temperatures (Fig. 8a). Not only the elution pH, but also the FC/EC selectivity was temperature-dependent. At lower temperatures (ice bath (~ 0 °C) and 10 °C), selectivity was increased, and efficiency was reduced compared to 25 °C. This agrees with the temperature-dependent diffusion coefficient and viscosity: at ambient temperatures, an increase

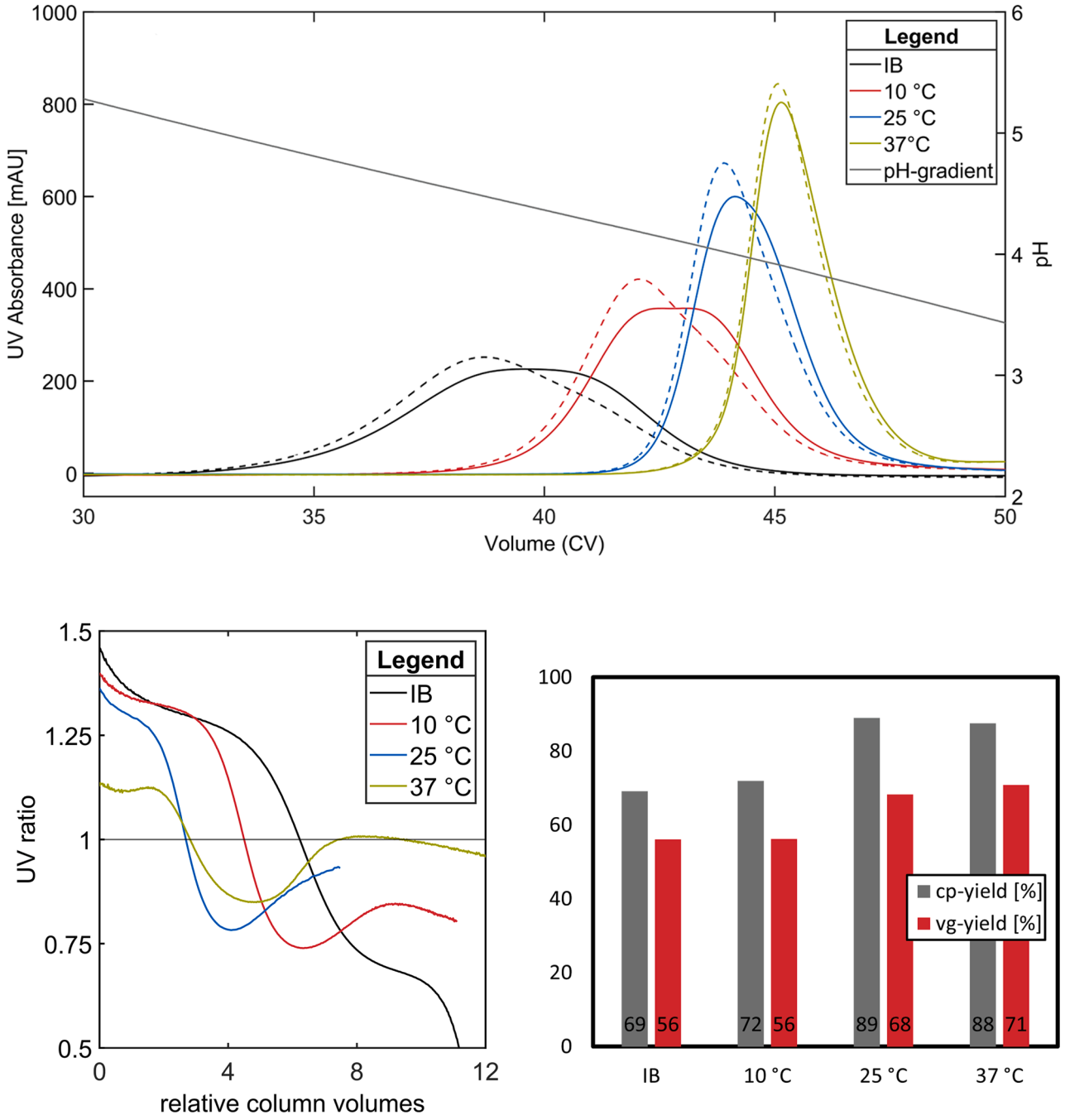

Fig. 8. Comparison of different temperatures (icebath (IB) ~ 0 °C, 10 °C, 25 °C, 37 °C) with AAV8 WT. Fig. 8a shows the pH-gradient (grey), and the elution peak for the respected temperature with 260 nm (–) and 280 nm (–). Fig. 8b shows the corresponding UV-ratios from 10 mAU-10 mAU. Relative column volumes are defined as the column volumes of the elution peak from 10 mAU to 10 mAU.

in temperature will increase diffusion of analytes within the column and impact the mass transfer between stationary and mobile phase as well as the viscosity, which decreases at higher temperatures, causing peak sharpening [53]. Close towards the end of the elution peak, the UV-ratio increased again for the investigated temperatures except 0 °C (Fig. 8b), suggesting that more FCs eluted again. This trend has been shown in Fig. 1 and was so far only observed for AAV8 WT on AAVX-resin. Process yields were lower at ice bath and 10 °C elution conditions compared to 25 °C and 37 °C (Fig. 8c).

Notably, we found a non-linear relation between elution temperature, elution pH, FC/EC selectivity and efficiency. To increase process robustness, future experiments should be performed in a temperature-controlled environment. At larger scale, in addition to the column, the buffers should be kept at the desired temperature to avoid process deviations. In our laboratory scale experiments with low flow rates and high relative surface areas of all tubing, it was sufficient to limit temperature control to column inlet and the column.

3.4. Relative hydrophobicity and charge differences

Charge differences between FCs and ECs as well as between different serotypes were determined in a pH-gradient on a Sartorius CIMac AAV empty/full analytical AEX column. While an isoelectric point cannot be determined with AEX-resin, as separation is based on the surface charge

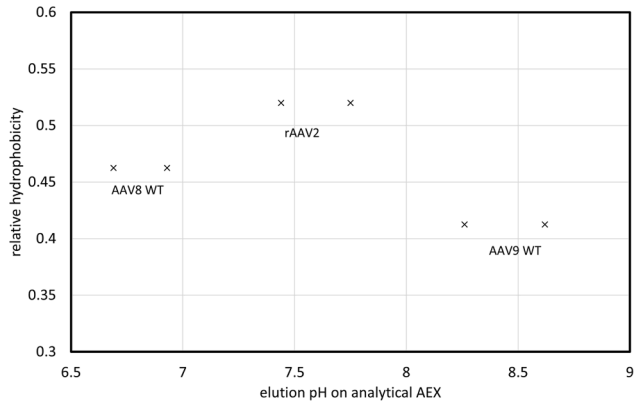

Fig. 9. relative hydrophobicities and charge differences of the respective serotypes were determined by HPLC as explained in Section 2.2.3. The values shown were obtained at the respective peak apex.

at given pH and ionic strength, the values obtained are useful to determine relative charge differences. The elution condition was determined at the respective peak apex. As reported in many studies before, full capsids have higher binding strength to AEX-resin than empty capsids, caused by the genomic DNA in a not fully elucidated mechanism [54]. All serotypes used in this study contained a genome of similar length and composition. The charge difference between full and empty capsids was similar between serotypes tested, in the range of 0.3 – 0.4 pH-units (Fig. 9). However, the capsid elution on a CIMac AAV full/empty column with pH-gradient did not correspond to the elution behavior on AAVX-resin. While on AAVX-resin the elution order was AAV9 WT, AAV8 WT, rAAV2 by decreasing pH, on AEX-resin it was AAV9 WT, then rAAV2 and AAV8 WT last. We conclude that the elution pH of different serotypes on affinity-resins cannot be predicted by the method applied here.

Capsids were furthermore analyzed for their respective relative hydrophobicity according to previous work with antibodies [55]. The relative hydrophobicity was determined by the retention time in a salt gradient with 0 being the lowest relative hydrophobicity and 1 being the highest, the elution point was determined at the elution peak apex, as explained in Section 2.2.3. It is shown in Fig. 9 that the analyzed capsids eluted in the range of 0.41 (AAV9 WT, least hydrophobic) to 0.52 (rAAV2, most hydrophobic). As previously shown, it was not possible to separate ECs and FCs solely by hydrophobic interactions [56]. However, the information obtained with these experiments can be helpful to analyze the susceptibility of different serotypes towards the salt concentration in the elution buffer during capture. While not in the scope of this work, purification of serotypes with a higher relative hydrophobicity can be expected to be influenced more strongly by the concentration and type of salt as well as temperature.

Experiments with atomic force microscopy revealed differences in hydrophobic binding strength depending not just on the serotype, but also on the presence or absence of a genome [57]. Since we were not able to separate full and empty capsids based on hydrophobicity on an analytical HIC-column, the necessary resolution potentially was not achieved as the reported differences in binding strength are minor. However, in our experiments the FC/EC selectivity weakly depended on temperature and salt molarity, two factors that modulate hydrophobic interactions. The main difference is the binding mechanism, as analytical Ether-5PW resin does not have affinity to one defined location on the capsid but rather to hydrophobic areas, whereas the observations made with camelid-derived ligands link to the specific binding site on the capsid's outer surface. The main effect of both higher temperature and increased salt molarity was an increase in binding strength that resulted in a more acidic elution pH. Both variables also impacted the FC/EC selectivity. From ice bath to 25 °C, the selectivity was unaltered, but it was diminished at 37 °C, possibly due to increased molecular motion or masking of electrostatic differences by strong hydrophobic forces. While the absence of NaCl resulted in reduced selectivity, molarities above 200 mM did not yield any further improvement.

4. Conclusion

Here we present an optimized method that unexpectedly increased selectivity for full AAV-capsids. This method utilizes commercially available affinity resins such as POROS™ CaptureSelect™ AAVX and can be implemented easily without the introduction of an additional unit operation. While this work focusses on the comparison of different serotypes, affinity resins and elution conditions in a linear gradient, further process development for manufacturing should include one or several pH-steps to simplify the process and increase robustness. The pH of the elution step for FC-capture is a sensitive tool that offers a tradeoff of yield and purity. While it has been shown that capture alone is not sufficient to reduce process-related impurities to an acceptable level, in combination with a second chromatographic unit operation such as polishing on AEX-resin, this method is a powerful tool that unlocks more control in a unit operation that is already widely used in industrial AAV purification.

CRediT authorship contribution statement

Lukas Bongers: Writing – review & editing, Writing – original draft, Visualization, Validation, Supervision, Methodology, Investigation, Formal analysis, Data curation, Conceptualization. **Linda E. Franken:** Validation, Investigation. **Dominik Hoch:** Investigation. **Veronika E. Huber:** Investigation. **Veronika Öttl:** Investigation. **Elena B. Raaf:** Investigation. **Jürgen Hubbuch:** Writing – review & editing, Supervision, Project administration. **Roberto Falkenstein:** Writing – review & editing, Validation, Supervision, Project administration, Methodology, Conceptualization. **Andres D. Martinez:** Writing – review & editing, Validation, Supervision, Project administration, Methodology, Conceptualization.

Declaration of competing interest

The authors declare the following financial interests/personal relationships which may be considered as potential competing interests:

Roberto Falkenstein, Andres Martinez, Elena B. Raaf have a patent pending to Roche Diagnostics GmbH. If there are other authors, they declare that they have no known competing financial interests or personal relationships that could have appeared to influence the work reported in this paper.

Acknowledgements

We would like to acknowledge Felix Wittkopp and Markus Haindl for funding and logistical support for this work.

Supplementary materials

Supplementary material associated with this article can be found, in the online version, at doi:10.1016/j.chroma.2025.466644.

Data availability

The authors do not have permission to share data.

References

[1] D. Wang, P.W.L. Tai, G. Gao, Adeno-associated virus vector as a platform for gene therapy delivery, Nat. Rev. Drug Discov. 18 (5) (2019) 358–378, https://doi.org/10.1038/s41573-019-0012-9.

[2] L.A. George, et al., Multiyear factor VIII expression after AAV gene transfer for hemophilia A, N. Engl. J. Med. 385 (21) (2021) 1961–1973, https://doi.org/10.1056/nejmoa2104205.

[3] L.A. Anderson, "How much does Elevidys cost?" [Online]. Available: https://www.drugs.com/medical-answers/how-elevidys-cost-3577480/.

[4] N. Brument, et al., A versatile and scalable two-step ion-exchange chromatography process for the purification of recombinant adeno-associated virus serotypes-2 and -5, Mol. Ther. 6 (5) (2002) 678–686, https://doi.org/10.1006/mthe.2002.0719.

[5] T. Tomono, et al., Ultracentrifugation-free chromatography-mediated large-scale purification of recombinant adeno-associated virus serotype 1 (rAAV1), Mol. Ther. - Methods Clin. Dev. 3 (2016) 15058, https://doi.org/10.1038/mtm.2015.58.

[6] J. Smith, J. Grieger, R.J. Samulski, Overcoming bottlenecks in AAV manufacturing for gene therapy, Cell Gene Ther. Insights. 4 (8) (2018) 815–825, https://doi.org/10.18609/cgti.2018.083.

[7] N. Jarvi, K. Hofman, A. Venkatesh, E. Gorecki, S.V. Balu-Iyer, Immunogenicity risk assessment of empty capsids present in adeno-associated viral vectors using predictive innate immune responses, J. Pharm. Sci. 113 (12) (2024) 3457–3469, https://doi.org/10.1016/j.xphs.2024.09.006.

[8] F. Mingozzi, et al., CD8+ T-cell responses to adeno-associated virus capsid in humans, Nat. Med. 13 (4) (2007) 419–422, https://doi.org/10.1038/nm1549.

[9] K. Gao, et al., Empty virions in AAV8 vector preparations reduce transduction efficiency and may cause total viral particle dose-limiting side effects, Mol. Ther. - Methods Clin. Dev. 1 (9) (2014) 9, https://doi.org/10.1038/mtm.2013.9.

[10] M. Urabe, et al., Removal of empty capsids from type 1 adeno-associated virus vector stocks by anion-exchange chromatography potentiates transgene expression, Mol. Ther. 13 (4) (2006) 823–828, https://doi.org/10.1016/j.ymthe.2005.11.024.

[11] B. Adams, H. Bak, A.D. Tustian, Moving from the bench towards a large scale, industrial platform process for adeno-associated viral vector purification, Biotechnol. Bioeng. 117 (10) (2020) 3199–3211, https://doi.org/10.1002/bit.27472.

[12] N. Laroudie, Q. Bazot, Advancing gene therapy development with a multi-serotype AAV affinity resin, Cell Gene Ther. Insights. 10 (02) (2024) 237–253, https://doi.org/10.18609/cgti.2024.036.

[13] O. Terova, S. Soltys, P. Hermans, J.D. Rooij, F. Detmers, Overcoming downstream purification challenges for viral vector manufacturing: enabling advancement of gene therapies in the clinic, Cell Gene Ther. Insights. 4 (2) (2018) 101–111, https://doi.org/10.18609/cgti.2018.017.

[14] M. Mietzsch, et al., Characterization of AAV-specific affinity ligands: consequences for vector purification and development strategies, Mol. Ther. - Methods Clin. Dev. 19 (2020) 362–373, https://doi.org/10.1016/j.omtm.2020.10.001.

[15] S. Kurth, et al., Separation of full and empty adeno-associated virus capsids by anion-exchange chromatography using choline-type salts, Anal. Biochem. 686 (2024) 115421, https://doi.org/10.1016/j.ab.2023.115421.

[16] G. Thakur, S. Mink, A.J. Garcia, H. Bak, A.D. Tustian, A two-pass anion-exchange chromatography strategy for enrichment of full capsids in manufacturing of adeno-associated viral vectors, Mol. Ther. Methods Clin. Dev. 33 (2) (2025) 101441, https://doi.org/10.1016/j.omtm.2025.101441.

[17] G. Qu, et al., Separation of adeno-associated virus type 2 empty particles from genome containing vectors by anion-exchange column chromatography, J. Virol. Methods 140 (1–2) (2007) 183–192, https://doi.org/10.1016/j.jviromet.2006.11.019.

[18] T.P. Wörner et al., "Adeno-associated virus capsid assembly is divergent and stochastic," *bioRxiv*, p. 2020.10.09.332619, 2020, doi: 10.1101/2020.10.09.332619.

[19] N. Ibreljic, B.E. Draper, C.W. Lawton, Recombinant AAV genome size effect on viral vector production, purification, and thermostability, Mol. Ther. Methods Clin. Dev. 32 (1) (2024) 101188, https://doi.org/10.1016/j.omtm.2024.101188.

[20] A.R. Giles, et al., Deamidation of amino acids on the surface of adeno-associated virus capsids leads to charge heterogeneity and altered vector function, Mol. Ther. 26 (12) (2018) 2848–2862, https://doi.org/10.1016/j.ymthe.2018.09.013.

[21] S.A. Nass, et al., Universal method for the purification of recombinant AAV vectors of differing serotypes, Mol. Ther. Methods Clin. Dev. 9 (2017) 33–46, https://doi.org/10.1016/j.omtm.2017.12.004.

[22] P.R.H. Joshi, A. Bernier, P.D. Moço, J. Schrag, P.S. Chahal, A. Kamen, Development of a scalable and robust AEX method for enriched rAAV preparations in genome-containing VCs of serotypes 5, 6, 8, and 9, Mol. Ther. Methods Clin. Dev. 21 (2021) 341–356, https://doi.org/10.1016/j.omtm.2021.03.016.

[23] W. Di, K. Koczera, P. Zhang, D.P. Chen, J.C. Warren, C. Huang, Improved adeno-associated virus empty and full capsid separation using weak partitioning multi-column AEX chromatography, Biotechnol. J. 19 (1) (2024) e2300245, https://doi.org/10.1002/biot.202300245.

[24] M. Florea, et al., High-efficiency purification of divergent AAV serotypes using AAVX affinity chromatography, Mol. Ther. - Methods Clin. Dev. 28 (2023) 146–159, https://doi.org/10.1016/j.omtm.2022.12.009.

[25] G.D. Florencio, G. Precigout, C. Beley, P.-O. Buclez, L. Garcia, R. Benchaouir, Simple downstream process based on detergent treatment improves yield and in vivo transduction efficacy of adeno-associated virus vectors, Mol. Ther. - Methods Clin. Dev. 2 (2015) 15024, https://doi.org/10.1038/mtm.2015.24.

[26] A.L. Gimpel, et al., Analytical methods for process and product characterization of recombinant adeno-associated virus-based gene therapies, Mol. Ther. Methods Clin. Dev. 20 (2021) 740–754, https://doi.org/10.1016/j.omtm.2021.02.010.

[27] W. Koehnlein, A. Holzgreve, K. Schwendner, R. Skudas, F. Schelter, Purification of hydrophobic complex antibody formats using a moderately hydrophobic mixed mode cation exchange resin, J. Chromatogr. A 1687 (2023) 463696, https://doi.org/10.1016/j.chroma.2022.463696.

[28] C. Wang, et al., Developing an Anion exchange chromatography assay for determining empty and full capsid contents in AAV6.2, Mol. Ther. Methods Clin. Dev. 15 (2019) 257–263, https://doi.org/10.1016/j.omtm.2019.09.006.

[29] O. Khanal, V. Kumar, M. Jin, Adeno-associated viral capsid stability on anion exchange chromatography column and its impact on empty and full capsid separation, Mol. Ther. Methods Clin. Dev. 31 (2023) 101112, https://doi.org/10.1016/j.omtm.2023.101112.

[30] F. Kröner, J. Hubbuch, Systematic generation of buffer systems for pH gradient ion exchange chromatography and their application, J. Chromatogr. A 1285 (2013) 78–87, https://doi.org/10.1016/j.chroma.2013.02.017.

[31] M. Mietzsch, et al., Improved genome packaging efficiency of adeno-associated virus vectors using Rep hybrids, J. Virol. 95 (19) (2021), https://doi.org/10.1128/jvi.00773-21 e00773-21.

[32] W.S. Kish, et al., Removal of empty capsids from high-dose adeno-associated virus 9 gene therapies, Biotechnol. Bioeng. 121 (8) (2024) 2500–2523, https://doi.org/10.1002/bit.28737.

[33] F. Destro, et al., The state of technological advancement to address challenges in the manufacture of rAAV gene therapies, Biotechnol. Adv. 76 (2024) 108433, https://doi.org/10.1016/j.biotechadv.2024.108433.

[34] J.K. Lorek, M. Isaksson, B. Nilsson, Chromatography in downstream processing of recombinant adeno-associated viruses: a review of current and future practises, Biotechnol. Bioeng. 122 (5) (2025) 1067–1086, https://doi.org/10.1002/bit.28932.

[35] Y. Xie, M. Butler, Multi-attribute analysis of adeno-associated virus by size exclusion chromatography with fluorescence and triple-wavelength UV detection, Anal. Biochem. 680 (2023) 115311, https://doi.org/10.1016/j.ab.2023.115311.

[36] J. ürg M. Sommer, et al., Quantification of adeno-associated virus particles and empty capsids by optical density measurement, Mol. Ther. 7 (1) (2003) 122–128, https://doi.org/10.1016/s1525-0016(02)00019-9.

[37] T.M. Leibiger, L. Min, K.H. Lee, Quantitative proteomic analysis of residual host cell protein retention across adeno-associated virus affinity chromatography, Mol. Ther. Methods Clin. Dev. 32 (4) (2024) 101383, https://doi.org/10.1016/j.omtm.2024.101383.

[38] O.F. Duzenli, G. Aslanidi, Consecutive affinity and ion-exchange chromatography for AAV9 vectors purification, Biomedicines. 13 (2) (2025) 361, https://doi.org/10.3390/biomedicines13020361.

[39] X. Tadeo, B. López-Méndez, D. Castaño, T. Trigueros, O. Millet, Protein stabilization and the Hofmeister effect: the role of hydrophobic solvation, Biophys. J. 97 (9) (2009) 2595–2603, https://doi.org/10.1016/j.bpj.2009.08.029.

[40] A.M. Hyde, S.L. Zultanski, J.H. Waldman, Y.-L. Zhong, M. Shevlin, F. Peng, General principles and strategies for salting-out informed by the Hofmeister Series, Org. Process. Res. Dev. 21 (9) (2017) 1355–1370, https://doi.org/10.1021/acs.oprd.7b00197.

[41] R.A. Lavoie, et al., Enrichment of adeno-associated virus serotype 5 full capsids by anion exchange chromatography with dual salt elution gradients, Biotechnol. Bioeng. 120 (10) (2023) 2953–2968, https://doi.org/10.1002/bit.28453.

[42] J.F. Wright, et al., Identification of factors that contribute to recombinant AAV2 particle aggregation and methods to prevent its occurrence during vector purification and formulation, Mol. Ther. 12 (1) (2005) 171–178, https://doi.org/10.1016/j.ymthe.2005.02.021.

[43] L. Motabar, et al., Impact of electrostatics on the aggregation, genome release, and self-interactions of AAV9 capsids, J. Pharm. Sci. 114 (9) (2025) 103899, https://doi.org/10.1016/j.xphs.2025.103899.

[44] G.A. Rodrigues, E. Shalaev, T.K. Karami, J. Cunningham, N.K.H. Slater, H. M. Rivers, Pharmaceutical development of AAV-based gene therapy products for the eye, Pharm. Res. 36 (2) (2019) 29, https://doi.org/10.1007/s11095-018-2554-7.

[45] A. Ismail et al., "Impact of low pH affinity chromatography elution on AAV transduction," Jan. 2025.

[46] M. Mietzsch, M. Kamat, K. Basso, P. Chipman, J.T. Huiskonen, R. McKenna, Structural characterization and epitope mapping of the AAVX affinity purification ligand, Mol. Ther. - Methods Clin. Dev. 32 (4) (2024) 101377, https://doi.org/10.1016/j.omtm.2024.101377.

[47] N.E. Clark, Structural basis of AAV affinity chromatography: from design to Cryo-EM validation [Online]. Available, https://www.repligen.com/Products/Resins/avipure/Poster%20-%202024%20Recovery%20, 2023, Structural%20basis%20of%20AAV%20affinity%20chrom.pdf.

[48] B. Gerlach, J.A. Kleinschmidt, B. Böttcher, Conformational changes in Adeno-associated virus type 1 induced by genome packaging, J. Mol. Biol. 409 (3) (2011) 427–438, https://doi.org/10.1016/j.jmb.2011.03.062.

[49] M. Mietzsch, et al., Comparative analysis of the capsid structures of AAVrh.10, AAVrh.39, and AAV8, J. Virol. 94 (6) (2019), https://doi.org/10.1128/jvi.01769-19, p. 10.1128/jvi.01769-19,.

[50] N.T. Southall, K.A. Dill, A.D.J. Haymet, A view of the hydrophobic effect, J. Phys. Chem. B 106 (10) (2002), https://doi.org/10.1021/jp020104r, 2812–2812.

[51] C.C. Miller, The Stokes-Einstein law for diffusion in solution, Proc. R. Soc. Lond. Ser. A, Contain. Pap. A Math. Phys. Character 106 (740) (1924) 724–749, https://doi.org/10.1098/rspa.1924.0100.

[52] E. van Dijk, A. Hoogeveen, S. Abeln, The hydrophobic temperature dependence of amino acids directly calculated from protein structures, PLoS. Comput. Biol. 11 (5) (2015) e1004277, https://doi.org/10.1371/journal.pcbi.1004277.
[53] T. Teutenberg, Potential of high temperature liquid chromatography for the improvement of separation efficiency—a review, Anal. Chim. Acta 643 (1–2) (2009) 1–12, https://doi.org/10.1016/j.aca.2009.04.008.
[54] C.L. Heldt, M.A. Skinner, G.S. Anand, Structural changes likely cause chemical differences between empty and full AAV capsids, Biomedicines. 12 (9) (2024) 2128, https://doi.org/10.3390/biomedicines12092128.
[55] W. Koehnlein, E. Kastenmueller, T. Meier, T. Treu, R. Falkenstein, The beneficial impact of kosmotropic salts on the resolution and selectivity of protein A chromatography, J. Chromatogr. A 1715 (2024) 464585, https://doi.org/10.1016/j.chroma.2023.464585.
[56] A. Rodriguez, A. Banazadeh, A. Ali, R. Singh, C. Zhou, Limitation of anion exchange chromatography and potential application of hydrophobic interaction chromatography for monitoring AAV9 capsid degradation upon thermal stress, J. Pharm. Sci. 114 (2) (2025) 983–989, https://doi.org/10.1016/j.xphs.2024.11.005.
[57] C.L. Heldt, O. Areo, P.U. Joshi, X. Mi, Y. Ivanova, A. Berrill, Empty and full AAV capsid charge and hydrophobicity differences measured with single-particle AFM, Langmuir. 39 (16) (2023) 5641–5648, https://doi.org/10.1021/acs.langmuir.2c02643.